1121
55

NATIONAL ADVISORY COMMITTEE FOR AERONAUTICS

TECHNICAL NOTE

No. 1122

SIDESLIP ANGLES AND VERTICAL-TAIL LOADS IN ROLLING PULL-OUT MANEUVERS

By Maurice D. White, Harvard Lomax, and Howard L. Turner

Ames Aeronautical Laboratory
Moffett Field, Calif.

Washington
April 1947

ERRATA

NACA TN 1122

SIDESLIP ANGLES AND VERTICAL-TAIL LOADS IN ROLLING PULL-OUT MANEUVERS

By Maurice D. White, Harvard Lomax, and Howard L. Turner

April 1947

In the original derivation of appendixes A and B, the load factor n was inappropriately included in the definition of τ. The following changes should be noted:

Page 4, change τ aerodynamic time $[(\rho V S_W/nm)t]$
to τ aerodynamic time $[(\rho V S_W/m)t]$

Pages 15 to 24, change $n\mu$ to μ.

Page 20 equation B5 first line, change $\int_0^{t/n}$ to $\int_0^{t}$

Page 20 equation B5 third line, delete $\frac{1}{n}$

Page 20 equation B5 fourth line, delete n.

Page 20 sixth line, change $b_1 \approx \sqrt{N_\beta n}$ to $b_1 \approx \sqrt{N_\beta}$

Figure 4, change $n\mu$ to μ.

The section "Design Charts" should be interpreted in accordance with the implications of the above changes. In particular, the distinctions made between $n\mu$ and μ are no longer pertinent.

NACA-Langley - 2-14-51 - 900

NATIONAL ADVISORY COMMITTEE FOR AERONAUTICS

TECHNICAL NOTE NO. 1122

SIDESLIP ANGLES AND VERTICAL-TAIL LOADS IN ROLLING PULL-OUT MANEUVERS

By Maurice D. White, Harvard Lomax, and Howard L. Turner

SUMMARY

Previous NACA reports have indicated that it is possible to develop angles of sideslip which may cause critical vertical-tail loads in abrupt rudder-fixed rolls from accelerated flight, but the reliability of methods for predicting these sideslip angles has not been demonstrated. In this report expressions for calculating the sideslip angles in these maneuvers are derived from theoretical considerations, and numerical solutions are obtained for a wide enough range of variables to permit construction of design charts. Comparison of the maximum sideslip angles obtained from the design charts and from flight tests with those obtained using a greatly simplified expression indicates sufficiently close agreement to warrant use of the simplified expression for first approximations in predicting sideslip angles and vertical-tail loads occurring in rolling pull-out maneuvers for conventional ailerons. An approximate method for treating cases of nonlinear directional-stability characteristics is presented which gives reasonably good results. The vertical-tail loads measured on one airplane in rolling pull-out maneuvers corresponded closely with those calculated by the simplest methods when the actual sideslip angles attainod were applied.

INTRODUCTION

Recently attention has been directed to the rolling pull-out maneuver as a condition in which crtical loads might be developed on the vertical tail through the attainment of large sideslip angles (reference 1). Subsequent flight tests have verified the fact that the vertical-tail loads in rolling pull-out maneuvers may exceed design loads based on other maneuvers. To indicate the order of magnitude of these loads approximate expressions were presented in reference 1 for estimating the maximum sideslip angles and maximum vertical-tail loads developed in this maneuver; it was indicated in reference 1, however, that flight values might exceed the values computed by these approximate expressions. Comparison of the sideslip angles determined in flight with those computed using the approximate expression of reference 1 verified that the approximate expression underestimates the sideslip angles developed, in most cases by a factor of the order of 2. This result indicated that the usefulness of the approximate expression of reference 1 is limited to the purpose of that report; that is, to demonstrate the importance of the rolling pull-out maneuver.

To provide information better suited to design purposes a more complete analysis has been made of the rolling-pull out maneuver. In the analysis a simplified expression suitable for preliminary design is developed for predicting the sideslip angle resulting from the rolling pull-out maneuver. Design charts which may be utilized for more precise computations are presented, and the effects of such factors as nonlinear directional-stability characteristics are discussed. Flight data are presented and compared with the analytical results.

The determination of vertical-tail loads in rolling pull-out maneuvers resolves itself essentially into the determination of the sideslip angles developed. This is demonstrated by the agreement shown in figure 1 between vertical-tail loads determined in flight and those computed by the simplest methods using measured values of sideslip angle, with no regard for sidewash effects, differences in the dynamic pressure at the tail from free-stream dynamic pressure, or possible yawing velocities. For this reason the present report is devoted exclusively to the determination of the sideslip angles developed in rolling pull-outs.

SYMBOLS

The following symbols are used throughout this report:

A aspect ratio (b_w^2/S_w)

a real part of complex root

b imaginary part of complex root

b_w wing span, feet

g acceleration due to gravity, 32.2 feet per second per second

I_X moment of inertia of airplane about X-axis, slug-feet square

I_Z moment of inertia of airplane about Z-axis, slug-feet square

i_a $4I_X/mb_w^2$

i_c $4I_Z/mb_w^2$

k_X radius of gyration about X-axis, feet

k_Z radius of gyration about Z-axis, feet

L_v load on vertical tail, pounds

l_t tail length, feet

m mass of airplane, slugs

n normal acceleration divided by acceleration of gravity

$\bar{p}$ rate of roll, radians per unit aerodynamic time

p rate of roll, radians per second

q free-stream dynamic pressure, pounds per square foot $\left(\frac{1}{2}\rho V^2\right)$

q_t dynamic pressure at tail, pounds per square foot

$\bar{r}$ rate of yaw, radians per unit aerodynamic time

r rate of yaw, radians per second

S_w wing area, square feet

S_t vertical-tail area, square feet

s operational parameter

t time, seconds

V velocity of airplane along flight path, feet per second

v component of flight velocity along Y-axis, feet per second

W weight of airplane, pounds

β angle of sideslip (positive when right wing is forward), radians

β^o angle of sideslip, degrees

δ_r rudder deflection, degrees

θ angle between horizontal plane and relative wind, radians

λ_n damping factor (used in $e^{\lambda_n t}$)

λ wing taper ratio $\left(\frac{\text{tip chord}}{\text{root chord}}\right)$

μ relative density coefficient $(m/\rho S_w b_w)$

ρ air density, slugs per cubic foot

τ aerodynamic time $[(\rho V S_w/m)t]$

τ_r relative rudder effectiveness $\left[\left(\partial C_{N_t}/\partial\delta_r\right)\left(\frac{1}{\partial C_{N_t}/\partial\alpha_t}\right)\right]$

φ angle of bank, radians

ψ angle of yaw, radians

L moment about X-axis, foot-pounds

N moment about Z-axis, foot-pounds

N_t normal force on vertical tail, pounds

Y force along Y-axis, pounds

C_{N_t} vertical tail normal force coefficient $(N_t/q_t S_t)$

$\partial C_{N_t}/\partial\alpha_t$ slope of curve of vertical-tail normal-force coefficient against angle of attack, per degree

C_L lift coefficient (nW/qS_W)

C_Y lateral force coefficient (Y/qS_w)

C_l rolling-moment coefficient $(L/qS_w b_w)$

ΔC_l increment of rolling-moment coefficient due to lateral-control deflection

C_n yawing-moment coefficient $(N/qS_w b_w)$

ΔC_n increment of yawing moment coefficient due to lateral-control deflection

C_{Y_β} $\partial C_Y/\partial\beta$

C_{l_β} $\partial C_l/\partial\beta$

C_{n_β}	$\partial C_n/\partial\beta$
C_{l_r}	$\partial C_l/\partial(rb_w/2V)$
C_{n_r}	$\partial C_n/\partial(rb_w/2V)$
C_{l_p}	$\partial C_l/\partial(pb_w/2V)$
C_{n_p}	$\partial C_n/\partial(pb_w/2V)$
Y_v	$(qS_w/mV)C_{Y_\beta}$
L_β	$(qS_wb_w/mk_X^2)C_{l_\beta}$
N_β	$(qS_wb_w/mk_Z^2)C_{n_\beta}$
N_p	$(qS_wb_w/mk_Z^2)(b_w/2V)C_{n_p}$
N_r	$(qS_wb_w/mk_Z^2)(b_w/2V)C_{n_r}$
L_p	$(qS_wb_w/mk_X^2)(b_w/2V)C_{l_p}$
L_r	$(qS_wb_w/mk_X^2)(b_w/2V)C_{l_r}$

$$\left.\begin{array}{l}\beta^* \\ \left(C_{n_\beta}{}^{o}\right)_1 \\ \left(C_{n_\beta}{}^{o}\right)_2\end{array}\right\}$$ parameters used in computing β^{o}_{max} for nonlinear curves of C_n against β

THEORETICAL ANALYSIS

For the purposes of the theoretical analysis the rolling pull-out maneuver is considered to consist of an abrupt aileron deflection in accelerated flight, the rudder being held fixed. The normal acceleration and the aileron deflection are considered constant throughout the maneuver, and the angle θ between the horizontal plane and the relative wind is considered small enough so that $\cos\theta$ can be set equal to unity. These assumptions are conservative in that they will result in computed sideslip angles larger than those that would be obtained in actual flight maneuvers where a finite time is required to reach maximum normal acceleration or maximum aileron deflection or where the normal acceleration is unsteady or where the angle θ is large. The effect of differences in θ on the magnitude of the maximum computed angle of sideslip will be small, but the effect of unsteady normal acceleration may be larger, though still conservative.

In the analysis the parameter $(\Delta C_l/C_{l_p})(C_L/C_{n_\beta}{}^\circ)$ is substituted for the parameter $(pb/2V)(C_L/C_{n_\beta}{}^\circ)$ used in reference 1.

The equations and methods used in the theoretical analysis are given in detail in appendixes A, B, and C. Appendix A gives the equations for which numerical solutions are obtained in order to develop design charts. In appendix B a simplified expression is obtained for calculating the maximum sideslip angle developed in rolling pull-outs. Appendix C describes an approximation made for the gravity component of force on the airplane which permits its inclusion in the equations of motion as a linear factor.

Simplified Expression

The theoretical analysis presented in detail in appendix A and appendix B leads to the results plotted in figure 2 from which the following simplified expression for the maximum sideslip angle developed in rolling pull-out maneuvers is deduced:

$$\frac{\beta^\circ_{max}}{(\Delta C_l/C_{l_p})(C_L/C_{n_\beta}{}^\circ)} = 1/4 \tag{1}$$

In the derivation of this expression the value of C_{n_p} was assumed as $C_L/16$. This value is about the mean of the values of $C_L/18$ and $C_L/14$ which would be deduced for aspect ratios of 6 and 10 and a taper ratio of 0.5 from reference 2. The relative insensitivity of this value to changes in both aspect ratio and taper ratio within current design limits is noteworthy. The values of C_{l_p} presented in reference 2 are based on lifting-line theory; refinements to these values based on lifting-surface theory are shown in reference 4.

In the development of equation (1), it was also assumed that the adverse yawing-moment coefficient of the ailerons was given by

$$\Delta C_n = (\Delta C_l/C_{l_p})(C_L/16)$$

This is the theoretical value for a wing of aspect ratio 8 and taper ratio 0.5 having ailerons extending over the outer 50 percent of the span, as obtained by combining data in references 2 and 3. These references may also be used to determine values of ΔC_n for other wing-aileron configurations.

In reference 3 only the induced yawing moment due to the ailerons is considered. For large aileron deflections or for unconventional ailerons the profile drag effect may also be important. An expanded form of equation (1) which may be used to account for small differences in ΔC_n from that assumed for equation (1) is given by equation (2).

$$\frac{\beta^{o}_{max}}{(\Delta C_l/C_{l_p})(C_L/C_{n_\beta}{}^{o})} = 2\,\frac{\Delta C_n}{C_L}\left(\frac{C_{l_p}}{\Delta C_l}\right) + \frac{1}{8} \qquad (2)$$

For reasons discussed in more detail later, the validity of equation (2) decreases as the value of ΔC_n departs from $(\Delta C_l/C_{l_p})(C_L/16)$.

The sum of the values of C_{n_p} and ΔC_n used in deriving equation (1) is equal to that used in deriving the equivalent expression given in reference 1. The value of the constant 1/4 given in equation (1) is, however, twice that obtained in reference 1, which indicates that the derivation of reference 1 which is based on static conditions is over-simplified.

In the next section of this report, Design Charts, the results of a more exact analysis indicate that equations (1) and (2), while satisfactory for the preliminary design of airplanes with conventional arrangements, may be greatly in error for airplanes with unconventional lateral-control devices such as spoilers.

Design Charts

In order to provide data suitable for design purposes, and to show by comparison the applicability of equations (1) and (2), a numerical analysis was made in which the maximum sideslip angle developed for each of several combinations of variables was determined. The equations of appendix A used for the analysis involve only minor assumptions and these are such as to result in slightly larger computed angles of sideslip than would actually be obtained.

The range of variables considered covers the limits of conventional design practice. The analysis was made for the conditions of the V-n diagram shown in figure 3. Calculations were made for the curve of $C_L = 0.9$ (curve A-B in fig. 3) and at a high-speed point for $n = 8$ (point C in fig. 3). Results obtained from this analysis are considered equally applicable to the region within the boundary shown in figure 3. Compressibility effects are not considered in the analysis.

Along the normal acceleration-velocity curve, values of $n\mu$ of 30, 75, and 120 were considered for a C_L of 0.9 and of 120 for a C_L of 0.35. The value of μ for an airplane with a wing loading of 40 pounds per square foot and a span of 40 feet at sea level is about 13. Variations in the other parameters such as vertical-tail size, dihedral effect, moment of inertia about the airplane X- and Z-axes, and wing aspect ratio and taper ratio were considered either individually or in combination where it appeared advisable. The combinations of parameters used in these computations are given in table I. Since the analysis was carried out on a dimensionless basis, the velocity and normal acceleration for any particular airplane configuration may be calculated from the expression

$$V = 8.02 \sqrt{\frac{n\mu b_W}{C_L}} \text{ feet per second}$$

$$n = 32.2 \frac{\rho b_W}{(W/S_W)} (n\mu)$$

In cases where the oscillations were divergent the maximum value of the sideslip angle was considered to be that attained in the first peak.

The results of the numerical analysis are presented in figures 4 and 5 in a form that permits easy interpolation for design purposes. The curves of figure 4 cover the part of the V-n diagram which is limited by maximum lift coefficient (curve A-B of fig. 3). In figure 4(a) the variation of β°_{max} with $(\Delta C_l/C_{l_p})(C_L/C_{n_\beta}{}^{\circ})$ is presented for various values of $C_{n_\beta}{}^{\circ}$, ΔC_n, and $n\mu$ for a value of $C_{l_\beta}{}^{\circ} = -0.0010$; corresponding data for a value of $C_{l_\beta}{}^{\circ} = 0$ are shown in figure 4(b).

Similar curves for very high speeds and high normal acceleration (point C of fig. 3) are shown in figure 5. For purposes of comparison, β°_{max} as calculated from equation (2) with ΔC_n set equal to $(\Delta C_l/C_{l_p})(C_L/16)$ is shown on all the curves. Also the results of applying equation (2) to the case of $\Delta C_n = 0$ is indicated in figure 4 for comparison with the corresponding curves obtained from the numerical analysis.

The curves of figure 4 indicate that for preliminary estimates of sideslip angles and corresponding vertical-tail loads the use of equation

(2) for values of ΔC_n around $(\Delta C_l/C_{l_p})(C_L/16)$, that is, equation (1), is satisfactory, the percentage error being for most practical configurations of a relatively low magnitude and the direction of the error being conservative except for arrangements having low dihedral effect and low directional stability. The deviations in the latter case are greatest for the lowest values of $n\mu$ where, from the standpoint of vertical-tail loads, the importance of the deviations would be less, since low values of $n\mu$ represent low values of normal acceleration and hence of C_L which correspond to low values of β.

The agreement shown in figure 4 between the design charts and the curve representing equation (2) with $\Delta C_n = 0$ is poorer than the agreement shown with $\Delta C_n = (C_l/C_{l_p})(C_L/16)$. This poorer agreement results from the fact that equation (2) neglects a phase relationship that exists between the effects of ΔC_n and C_{n_p}. This phase relationship is properly accounted for only where $\Delta C_n = (C_l/C_{l_p})(C_L/16)$ as in equation (1), so that equation (2) becomes less valid as it departs from equation (1). The varying discrepancies indicated in figure 4 between the results of the numerical analysis and of the application of equations (1) and (2) may be used as an indication of the discrepancies that will arise from the use in equation (2) of other values of ΔC_n.

Results of applying the numerical analysis to high values of $n\mu$ and low values of C_L which together correspond to high speeds and high accelerations are shown in figure 5 and indicate that for this condition the use of equation (1) is decidedly conservative for all configurations. This condition is not considered too important as regards vertical-tail loads because the maximum amount of aileron control is generally not applied at the highest speeds, with the result that the loads are not critical at the highest speeds. These curves are included, however, as an indication of the range of applicability of equation (1).

The effects of independent changes in several other variables that were considered in the analysis are indicated in figure 6. The results in figure 6(a) indicate that, for the changes in configuration assumed, the differences are of secondary order. Figure 6(b) shows that the rate of movement of the aileron control within the limits indicated has only a small effect on the maximum sideslip angles attained.

Discussion of Nonlinear Characteristics

The preceding analysis has been carried out assuming linear variations of C_n with β° for all configurations. In practice, however, these curves as well as those for other stability coefficients are frequently nonlinear. Accordingly, an analysis was made to develop methods for handling nonlinear variations of C_n with β^o that would permit use of the simplified equations (1) and (2) or the design charts of figure 4. For this purpose numerical calculations were made of the maximum sideslip angles developed in rolling pull-outs, using the equations of appendix A, but modified by using appropriate initial conditions, and for simplicity, by using the angle of bank φ instead of the approximation of appendix C. For the calculations $C_{n_{\beta^o}}$ was assumed nonlinear, C_{n_r} and $C_{Y_{\beta^o}}$ were assumed to vary consistently with $C_{n_{\beta^o}}$; and all other parameters of the airplane remained constant. The various curves of C_n against β^o covered by the calculations are believed to encompass roughly the variations usually encountered in practice. The variations assumed are shown in figure 7 together with the results of the calculations presented as values of maximum sideslip angle attained for various applied rolling-moment coefficients ΔC_l. The parameter ΔC_l was used instead of $(\Delta C_l/C_{l_p})(C_L/C_{n_{\beta^o}})$ in the abscissa of figure 7 because for the nonlinear case no single value of $C_{n_{\beta^o}}$ could logically be used in the latter term.

The curves of figure 7 indicate that for the cases considered the variations of β^o_{max} with ΔC_l are consistent and may be predicted by the following purely empirical method:

1. Denote by $(C_{n_{\beta^o}})_1$ the slope of the curves of C_n against β^o through $\beta = 0$, by $(C_{n_{\beta^o}})_2$ the slope of the curve of C_n against β^o at values of β^o beyond the break in the curve and by β^* the sideslip angle at which the break in the curve of C_n against β^o occurs.

2. Assuming each of the slopes $(C_{n_{\beta^o}})_1$ and $(C_{n_{\beta^o}})_2$ to exist separately through $\beta = 0$, compute the curves of β^o_{max} against $(\Delta C_l/C_{l_p})(C_L/C_{n_{\beta^o}})$ from the design charts.

3. Through $\beta = 0$ draw the curve of β^o_{max} against ΔC_l corresponding to $(C_{n_{\beta^o}})_1$. Denote this curve as line A.

4. Through $\beta^o = 1.5\beta^* \left[1 - (C_{n_{\beta^o}})_1/(C_{n_{\beta^o}})_2 \right]$ at $\Delta C_l = 0$, draw the curve of β^o_{max} against ΔC_l corresponding to $(C_{n_{\beta^o}})_2$. Denote this curve as line B.

The final curve is composed then of line A from $\beta = 0$ to the intersection of lines A and B, and of line B from the intersection on to higher values of β^o. The curves computed from this method for curves II, IV, and V are shown in figure 7 for comparison with those computed by the numerical analysis. A reasonable fairing of the intersection of lines A and B may be applied for greater accuracy.

This analysis was made only for curves of C_n against β° which could be approximated by two straight lines. For cases in which this is not sufficient, or for cases in which extreme accuracy is desired, solutions may be obtained by use of a differential analyzer or by a step-by-step integration as in reference 5.

The generality of the method presented and conclusions indicated by the curves of figure 7 is not, of course, established by the few cases considered. The results do offer promise that with further analysis the conclusions will be verified or other rational simplifications will be developed. In assessing the value of the methods given here it is of interest to note that it gave good agreement with the maximum sideslip angles computed for the airplane of reference 5 by step-by-step methods.

FLIGHT-TEST RESULTS

Flight data which may be compared with the theoretical results previously discussed have been obtained on two airplanes, one of which was flown with two different vertical-tail configurations. Views of the airplanes tested are shown in figure 8. A typical time history of a roll out of a steady turn is given in figure 9. It will be noted in figure 9 that the maximum value of the vertical-tail load occurs at the time of maximum sideslip. For airplane 1, Ames flight data obtained in aileron rolls were used, and for airplane 2 at configurations 1 and 2, Langley flight data on rolling pull-outs were used. For airplane 3, the maneuvers were not made steadily enough to permit correlation with the design charts or with equation (1), the normal acceleration for most runs being less steady than the time history shown in figure 9.

Comparison of Flight and Theoretical Data

For the airplanes for which flight data were available, there were insufficient data to permit accurate estimation of C_{l_β} or of C_{n_β} so that correlation could not justifiably be made with the design charts presented in the preceding sections of this report. As an indication of the applicability of equation (1), however, the value of C_{n_β} was estimated by the method shown in table II. The resulting sideslip angles are compared with values obtained in flight tests in figure 10. As a matter of interest the values of sideslip angle computed from the approximate expression of reference 1, that is,

$$\beta^{\circ} = \frac{C_L}{8} \frac{(pb_w/2V)}{(\partial C_n/\partial \beta^{\circ})} \tag{3}$$

are also shown in figure 10. For simplicity the change in sideslip angle denoted by $\Delta\beta^{\circ}$ is used in figure 10 instead of the absolute sideslip angle of β°.

For airplane 1, excellent agreement is indicated between flight data and equation (1) and correspondingly poor agreement for equation (3). (See fig. 10.)

For airplane 2 with configuration 1 the comparison indicates reasonably good agreement between flight values of β and values computed from equation (1).

For airplane 2 with configuration 2, the agreement between flight data and equation (1) is less favorable.

Although the data for airplane 3 were not steady enough to permit their inclusion in the correlation, it is of interest that when the maximum accelerations were used in the computations the values of sideslip angle were consistently larger than those obtained in flight.

There are several factors entering into the foregoing comparison that would explain, at least partially, the disagreements noted and which should be considered in the interpretation of all the comparisons. These factors, it will be noted, are essentially defects in the basic data and hence represent limitations in the application to these airplanes of the design charts as well as equation (1). One of these factors is the value of C_{n_β} used in the approximate expression. The method used for determining this value in the present case, noted in table II, involves the estimation of the values of $\partial C_{N_t}/\partial \alpha_t$ and τ_r from a knowledge of geometric properties of the airplane and of the value of $d\delta_r/d\beta$ as determined from steady sideslips. The methods used for estimating the values of $\partial C_{N_t}/\partial \alpha_t$ and τ_r are based on wind-tunnel data (reference 6) and remain to be verified by flight tests. For airplanes that are already flying, a preferable method of determining C_{n_β} from flight tests is indicated in reference 7.

In addition, the methods do not attempt to take into account rationally the possible nonlinearity of the curves of C_n against β which are frequently found in practice. This factor is discussed at length in a preceding section of this report. In this connection it is significant that the curves of δ_r versus β in steady sideslip were less linear for configuration 2 than for configuration 1 of airplane 2, and the agreement between flight and computed values of sideslip angle was not so good for configuration 2 as for configuration 1.

A third source of error results from the use of the term $(\Delta C_l / C_{l_p})(C_L/16)$ for the adverse yawing-moment coefficient of the ailerons. Aside from the small differences arising from differences in wing and aileron configurations from that assumed, the theoretical analysis from which this value was obtained (reference 2 combined with reference 3) accounts only for the induced drag and not for the profile drag due to aileron deflection which may in some cases be of significant value.

Vertical-Tail Loads

For airplane 3, the flight data were obtained at the Ames laboratory from simultaneous rudder-fixed pull-ups and rolls and from abrupt rudder-fixed rolls from steady accelerated turns. Both maneuvers were basically a sudden application of ailerons in accelerated flight and no differentiation is made between the data for the two maneuvers.

The maximum loads on the vertical tail as obtained from pressure-distribution measurements taken while performing these maneuvers are compared in figure 1 with those calculated using the expression

$$L_v = q_t S_t \frac{dC_{N_t}}{d\alpha_t} \beta^o \qquad (4)$$

The values of β^o and q_t used in the expression were flight values corresponding to the time at which the loads were obtained, and no allowance was made for the effects of sidewash as discussed in reference 8, and q_t was assumed equal to q. However, the data were corrected for the load changes resulting from small inadvertent movements of the rudder. At the time of maximum sideslip angle the tail loads computed in this manner gave good agreement with the measured loads; at other times in the runs as indicated in the time history of figure 9, effects of yawing velocity, and so forth, would have to be included to obtain correlation. The scatter indicated in figure 1 is partly accounted for by the accuracy with which the loads are determined (error estimated to be 5 to 15 percent, depending on the absolute magnitude of the load). It appears, therefore, that equation (4) is adequate for estimating vertical-tail loads when the correct sideslip angles are applied.

CONCLUSIONS

From a theoretical analysis of the motions of an airplane in a rudder-fixed, rolling pull-out maneuver and from comparison of the results of the analysis with flight data the following results have been obtained:

1. From numerical solutions to the theoretical equations design charts were developed for predicting the sideslip angles in rolling pull-outs for a wide range of variables.

2. A simplified expression for computing the maximum sideslip angles in rolling pull-outs was derived. The maximum sideslip angles computed by this expression were sufficiently close to those obtained from flight tests and from the design charts to warrant use of the expression for preliminary estimates of the maximum sideslip angles and hence the maximum vertical-tail loads.

3. An approximate method was developed for treating cases of non-linear directional-stability characteristics. From a limited comparison with results obtained from a numerical analysis of the theoretical expressions, the approximate method appeared to be generally applicable.

4. The vertical-tail loads in rolling pull-out maneuvers corresponded closely with those calculated by the simplest methods when the actual sideslip angles attained were applied.

Ames Aeronautical Laboratory,
National Advisory Committee for Aeronautics,
Moffett Field, Calif., August 1946.

APPENDIX A

EQUATIONS FOR NUMERICAL ANALYSIS

The solution to the linearized lateral equations of motion (reference 9)

$$C_l = \frac{I_x \ddot{\phi}}{qSb} = C_{l_p}\frac{pb}{2V} + C_{l_r}\frac{rb}{2V} + C_{l_\beta}\beta + C_{l_\delta}\delta_a$$

$$\left(\frac{d\bar{p}}{d\tau} - \bar{p}\frac{C_{l_p}}{i_a}\right) + \left(-\bar{r}\frac{C_{l_r}}{i_a}\right) + \left(-2\beta\frac{C_{l_\beta}}{i_a}\mu\right) = 2\Delta C_l\frac{\mu}{i_a}$$ Rolling Moment

$$C_n = \frac{I_z \ddot{\psi}}{qSb} = C_{n_p}\frac{pb}{2V} + C_{n_r}\frac{rb}{2V} + C_{n_\beta}\beta + C_{n_\delta}\delta_A$$

$$\left(-\bar{p}\frac{C_{n_p}}{i_c}\right) + \left(\frac{d\bar{r}}{d\tau} - \bar{r}\frac{C_{n_r}}{i_c}\right) + \left(-2\beta\frac{C_{n_\beta}}{i_c}\mu\right) = 2\Delta C_n\frac{\mu}{i_c}$$ Yawing Moment

$$C_Y = C_{Y_\beta}\beta = \frac{mV}{qS}\dot{\psi} + \frac{mV}{qS}\dot{\beta} - \frac{W}{qS}\sin\phi$$

$$\left(-\frac{1}{2}C_L\varphi\right) + (\bar{r}) + \left(\frac{d\beta}{d\tau} - \frac{1}{2}\beta C_{Y_\beta}\right) = 0 \qquad \text{(A1)}$$ Side Force

was obtained by operational methods using the Laplacian operator, such that (reference 10, p. 2)

$$\tilde{f}(s) = \int_0^\infty \bar{f}(x)\, e^{-sx}\, dx$$

$$s\tilde{f}(s) - \bar{f}(o) = \int_0^\infty \frac{d\bar{f}}{d\tau}\, e^{-sx}\, dx \qquad \text{(A2)}$$

The reduced equations, therefore, can be written,

$$\tilde{p}\left(s - \frac{C_{l_p}}{i_a}\right) - \tilde{r}\frac{C_{l_r}}{i_a} - 2\tilde{\beta}\frac{C_{l_\beta}\mu}{i_a} = 2\frac{\Delta C_l \mu}{s i_a}$$

$$\tilde{p}\left(-\frac{C_{n_p}}{i_c}\right) + \tilde{r}\left(s - \frac{C_{n_r}}{i_c}\right) - 2\tilde{\beta}\,\frac{C_{n_\beta}\mu}{i_c} = 2\,\frac{\Delta C_n\mu}{s i_c}$$

$$\tilde{p}\left(-\frac{C_L}{2s}\right) + \tilde{r} + \tilde{\beta}\left(s - \frac{1}{2}C_{Y_\beta}\right) = 0 \qquad \text{(A3)}$$

provided the initial rates of roll and yaw and the initial angles of bank, yaw, and sideslip are all zero. The solution to these equations in terms of angles of sideslip is given, therefore, by

$$\beta = L^{-1}\left\{\frac{\begin{vmatrix} \left(s - \frac{C_{l_p}}{i_a}\right) & \left(-\frac{C_{l_r}}{i_a}\right) & \left(2\,\frac{\Delta C_l\mu}{s i_a}\right) \\ \left(-\frac{C_{n_p}}{i_c}\right) & \left(s - \frac{C_{n_r}}{i_c}\right) & \left(2\,\frac{\Delta C_n\mu}{s i_c}\right) \\ \left(-\frac{C_L}{2s}\right) & (1) & (0) \end{vmatrix}}{\begin{vmatrix} \left(s - \frac{C_{l_p}}{i_a}\right) & \left(-\frac{C_{l_r}}{i_a}\right) & \left(-2\,\frac{C_{l_\beta}\mu}{i_a}\right) \\ \left(-\frac{C_{n_p}}{i_c}\right) & \left(s - \frac{C_{n_r}}{i_c}\right) & \left(-2C_{n_\beta}\,\frac{\mu}{i_c}\right) \\ \left(-\frac{C_L}{2s}\right) & (1) & \left(s - \frac{1}{2}C_{Y_\beta}\right) \end{vmatrix}}\right\} \qquad \text{(A4)}$$

where the symbol L^{-1} stands for the inverse of the operation indicated by equation (A2). The reduction of this expression is normally obtained by factoring the denominator of equation (A4) and making use of the expression

$$L^{-1}\left(\frac{1}{s-\lambda_n}\right) = e^{\lambda_n \tau} \qquad \text{(A5)}$$

In the present case, however, the denominator represents a quartic for which there is no practical general factorization, so that either a numerical solution or simplifying assumptions are required to obtain quantitative results in terms of the derivatives.

The design charts presented as figures 4 and 5 were obtained from numerical solutions using values of the derivatives presented in table I.

APPENDIX B

DERIVATION OF APPROXIMATE EXPRESSION

Neglecting the terms $\frac{1}{2}C_L$ and C_{n_p}/i_c in finding the roots to the quartic, an assumption which is best for high-speed unaccelerated flight, equation (A4) is written

$$\tilde{\beta} = \left\{ \frac{\begin{vmatrix} \left(s - \frac{C_{l_p}}{i_a}\right) & \left(-\frac{C_{l_r}}{i_a}\right) & \left(2\frac{\Delta C_l \mu}{s i_a}\right) \\ \left(-\frac{C_{n_p}}{i_c}\right) & \left(s - \frac{C_{n_r}}{i_c}\right) & \left(2\frac{\Delta C_n \mu}{s i_c}\right) \\ \left(-\frac{1}{2}C_L \frac{1}{s}\right) & (1) & (0) \end{vmatrix}}{\begin{vmatrix} \left(s - \frac{C_{l_p}}{i_a}\right) & \left(-\frac{C_{l_r}}{i_a}\right) & \left(-2\frac{C_{l_\beta}\mu}{i_a}\right) \\ (0) & \left(s - \frac{C_{n_r}}{i_c}\right) & \left(-2\frac{C_{n_\beta}\mu}{i_c}\right) \\ (0) & (1) & \left(s - \frac{1}{2}C_{Y_\beta}\right) \end{vmatrix}} \right\} \tag{B1}$$

This reduces to

$$\tilde{\beta} = \frac{-\left(s - \frac{C_{l_p}}{i_a} - \frac{\frac{1}{2}C_{l_r}C_L}{i_a s}\right) 2\frac{\Delta C_n \mu}{s i_c} + \left[-\frac{C_{n_p}}{i_c} + \frac{\frac{1}{2}C_L}{s}\left(s - \frac{C_{n_r}}{i_c}\right)\right] 2\frac{\Delta C_l \mu}{s i_a}}{\left[s - (C_{l_p}/i_a)\right](s - a - ib)(s - a + ib)} \tag{B2}$$

where

$$a \approx \frac{1}{2}\left[(C_{n_r}/i_c) + \frac{1}{2}C_{Y_\beta}\right]$$

and where, by further neglecting

$$[(C_{Y_\beta}/2) - (C_{n_r}/i_c)]^2/4$$

as compared to

$$2\pi(C_{n_\beta}\mu/i_c), \quad b \approx \sqrt{2\pi(C_{n_\beta}\mu/i_c)}$$

The part of equation (B2) multiplying $2\pi(\Delta C_n\mu/si_c)$ reduces to $-[s - (C_{l_p}/i_a)]$ since $\frac{1}{2}(C_{l_r}C_L/i_a)$ may be neglected as compared to C_{l_p}/i_a. This part can be rewritten

$$-\pi\frac{\Delta C_n\mu}{i_c ibs}\left(\frac{1}{s-a-ib} - \frac{1}{s-a+ib}\right)$$

which, according to equation (A5), has the inverse transform (reference 10)

$$-2\pi\frac{\Delta C_n\mu}{i_c b}\int_0^T e^{ax}\sin bx\,dx \tag{B3}$$

The part of equation (B1) which multiplies $2\pi(\Delta C_l\mu/i_a s)$ can be rewritten

$$2\pi\frac{\Delta C_l\mu}{si_a}\left(-\frac{C_{n_p}}{i_c} + \frac{1}{2}C_L - \frac{1}{2}C_L\frac{C_{n_r}}{si_a}\right)\left\{\frac{\left[\dfrac{1}{\left(\dfrac{C_{l_p}}{i_a} - a\right)^2 + b^2}\right]}{s - (C_{l_p}/i_a)}\right.$$

$$\left. + \frac{\left\{\dfrac{1}{2ib[a - (C_{l_p}/i_a) + ib]}\right\}}{s - a - ib} - \frac{\left\{\dfrac{1}{2ib[a - (C_{l_p}/i_a) - ib]}\right\}}{s - a + ib}\right\}$$

which, according to equation (A5), has the inverse transform

$$2\frac{\Delta C_{l}\mu}{i_a}\int_0^{T}\left[\frac{\frac{1}{2}C_L C_{n_r} i_a}{C_{l_p}(a^2+b^2)i_c} + \frac{-\frac{C_{n_p}}{i_c}+\frac{1}{2}C_L-\frac{1}{2}C_L\frac{C_{n_r}}{C_{l_p}}\frac{i_a}{i_c}}{[(C_{l_p}/i_a)-a]^2+b^2}\,e^{\frac{C_{l_p}}{i_a}x}\right.$$

$$+\frac{\frac{C_{n_p}}{i_c}-\frac{1}{2}C_L+\frac{C_L C_{n_r}}{2i_c}\left(\frac{2a-\frac{C_{l_p}}{i_a}}{a^2+b^2}\right)}{[(C_{l_p}/i_a)-a]^2+b^2}\,e^{ax}\cos bx$$

$$+\frac{\frac{1}{b}\left(\frac{C_{n_p}}{i_a}-\frac{1}{2}C_L\right)[(C_{l_p}/i_a)-a]}{[(C_{l_p}/i_a)-a]^2+b^2}\,e^{ax}\sin bx$$

$$\left.-\frac{(C_L C_{n_r}/2bi_c)\,[a^2-b^2-a(C_{l_p}/i_a)]\,/(a^2+b^2)}{[C_{l_p}/i_a)-a]^2+b^2}\,e^{ax}\sin bx\right]dx \qquad \text{(B4)}$$

By assuming now that $C_{n_p} = (C_L/16)$ and the adverse yawing-moment coefficient of the ailerons ΔC_n is equal to $(C_L/16)(\Delta C_l/C_{l_p})$, and changing the notation and the variable in order to simplify the results, the sum of equations (B3) and (B4) can be written

$C_{n_p}\frac{pb}{2V} = C_{n_{\delta_a}}\delta_a$??

$$\frac{\beta}{\left(\dfrac{\Delta C_{l}C_{L}}{C_{l_p}C_{n_\beta}}\right)} = \int_0^{t/4}\left\{\frac{1}{2}N_r i_c \frac{N_\beta}{a_1^2 + b_1^2} + \frac{\dfrac{L_pN_\beta}{16} + \dfrac{L_pN_\beta i_c}{2}\left(1 - \dfrac{N_r}{L_p}\right)}{(L_p - a_1)^2 + b_1^2} e^{L_p x}\right.$$

$$- \frac{\dfrac{1}{16} + \dfrac{1}{2}i_c\left[1 - N_r\left(\dfrac{2a_1 - L_p}{a_1^2 + b_1^2}\right)\right]}{(L_p - a_1)^2 + b_1^2} L_pN_\beta e^{a_1 x}\cos b_1 x$$

$$+ \frac{1}{b_1}\left[\frac{L_pb_1\left(\dfrac{-1}{16} - \dfrac{1}{2}i_c\right)\left(L_p - a_1\right) - \dfrac{1}{2}i_cN_rL_pb_1\left(\dfrac{a_1^2 - b_1^2 - a_1L_p}{a_1^2 + b_1^2}\right)}{(L_p - a_1)^2 + b_1^2}\right.$$

$$\left.\left. - \frac{1}{16}b_1\right] e^{a_1 x}\sin b_1 x\right\} dx \tag{B5}$$

where

$$a_1 \approx \frac{1}{2}(Y_v + N_r)$$

$$b_1 \approx \sqrt{N_\beta}$$

Equation (B5) may be written

$$\frac{\beta^{\circ}_{max}}{(\Delta C_{l}C_{L}/C_{l_p}C_{n_\beta}{}^{\circ})} = f(N_\beta,\ L_p,\ N_r,\ Y_v,\ i_c)$$

As an indication of the magnitude resulting from this analysis, the following approximate values were chosen:

$$N_r = -0.126 - 0.050\ N_\beta$$

$$Y_v = -0.177 - 0.012\ N_\beta$$

$$i_c = 0.143$$

and equation (B5) was plotted on figure 2 for various values of N_β and L_p. The curves show that for the assumption mentioned, equation (B5) may be written with little error as

$$\frac{\beta^o{}_{max}}{(\Delta C_l C_L / C_{l_p} C_{n_\beta}{}^o)} = \frac{1}{4}$$

APPENDIX C

APPROXIMATION FOR SINφ IN THEORETICAL ANALYSIS

The assumption made in solving equation (A1) that φ is equal to $\sin\varphi$ is equivalent to replacing the sine curve with a straight line having the same slope as the initial slope of the sine curve, and becomes increasingly erroneous as φ becomes greater. A better approximation may be obtained by finding the slope of a straight line which has the same integrated effect as the sine curve. This relationship may be expressed mathematically by

$$\int_0^{\tau_1} k\varphi d\tau = \int_0^{\tau_1} \sin\varphi\ d\tau$$

or

$$\int_0^{\tau_1} \varphi \left(k - \frac{\sin\varphi}{\varphi}\right) d\tau = 0 \qquad \text{(C1)}$$

where k represents the desired straight line slope and τ_1 is the time of maximum sideslip.

The angle of bank will certainly be greater than zero in the region considered and may be replaced by some average value Φ, so that equation (C1) can be written as

$$\Phi \int_0^{\tau_1} \left(k - \frac{\sin\varphi}{\varphi}\right) d\tau = 0$$

or

$$k = \frac{1}{\tau_1} \int_0^{\tau_1} \frac{\sin\varphi}{\varphi}\, d\tau \qquad \text{(C2)}$$

In order to solve equation (C2), an iteration process is used. That is, equation (A1) is solved with the original substitution of φ for $\sin\varphi$ to determine the variation of φ with τ and the value of τ_1. These values are used in equation (C2) and k is determined. This value of k is then multiplied into the term $\frac{1}{2}C_L\varphi$ of equation (A1) and equation (A1) is again solved, this time for β. This second iteration usually is sufficiently accurate for the evaluation of β_{max}; but if a check solution for φ and τ_1 shows that it is not sufficiently accurate, the process may be repeated.

REFERENCES

1. Gilruth, Robert R.: Analysis of Vertical-Tail Loads in Rolling Pull-Out Maneuvers. NACA CB No. L4H14, 1944.

2. Pearson, Henry A., and Jones, Robert T.: Theoretical Stability and Control Characteristics of Wings with Various Amounts of Taper and Twist. NACA Rep. No. 635, 1938.

3. Weick, Fred E., and Jones, Robert T.: Résumé and Analysis of NACA Lateral Control Research. NACA Rep. No. 605, 1937.

4. Swanson, Robert S., and Priddy, E. LaVerne: Lifting-Surface-Theory Values of the Damping in Roll and of the Parameter Used in Estimating Aileron Stick Forces. NACA ARR No. L5F23, 1945.

5. Wolowicz, Chester H.: Prediction of Motions of an Airplane Resulting from Abrupt Movement of Lateral or Directional Controls. NACA ARR No. L5E02, 1945.

6. Pass, H. R.: Analysis of Wind-Tunnel Data on Directional Stability and Control. NACA TN No. 775, 1940.

7. Bishop, Robert C., and Lomax, Harvard: A Simplified Method for Determining from Flight Data the Rate of Change of Yawing-Moment Coefficient with Sideslip. NACA TN No. 1076, 1946.

8. Recant, Isidore G., and Wallace, Arthur R.: Wind-Tunnel Investigation of the Effect of Vertical Position of the Wing on the Side Flow in the Region of the Vertical Tail. NACA TN No. 804, 1941.

9. Jones, Robert T.: A Study of the Two-Control Operation of an Airplane. NACA Rep. No. 579, 1937.

10. Churchill, Ruel V.: Modern Operational Mathematics in Engineering. McGraw-Hill Book Co., Inc., 1944.

TABLE I.– COMBINATIONS OF VARIABLES COVERED BY NUMERICAL ANALYSIS

Configuration	1	2	3	4	5	6	7	8	9	10	11[1]	12[1]	13
C_{l_p}	−0.455	−0.455	−0.455	−0.455	−0.455	−0.455	−0.455	−0.455	−0.430	−0.415	−0.455	−0.455	−0.455
C_{l_r}	.198	.198	.198	.198	.198	.198	.198	.198	.189	.180	.0578	.0578	.198
C_{l_β}	−.0573	−.0573	−.0573	0	0	0	−.0573	−.0573	−.0573	−.0573	−.1146	0	−.0573
C_{n_p}	−.0440	−.0440	−.0440	−.0440	−.0440	−.0440	−.0440	−.0440	−.0401	−.0525	−.0128	−.0128	−.0440
C_{n_r}	−.0669	−.0955	−.1580	−.0669	−.0955	−.1580	−.0955	−.0955	−.0982	−.0959	−.0669 −.0955 −.1580	−.0669 −.0955 −.1580	−.0955
C_{n_β}	.0229	.0515	.1030	.0229	.0515	.1030	.0515	.0515	.0515	.0515	.0229 .0515 .1030	.0229 .0515 .1030	.0515
C_{Y_β}	−.429	−.527	−.650	−.429	−.527	−.650	−.527	−.527	−.527	−.527	−.429 −.527 −.650	−.429 −.527 −.650	−.527
C_L	.9	.9	.9	.9	.9	.9	.9	.9	.9	.9	.35	.35	.9
i_a	.06	.06	.06	.06	.06	.06	.12	.06	.06	.06	.06	.06	.06
i_c	.16	.16	.16	.16	.16	.16	.16	.20	.16	.16	.16	.16	.16
μ	30 120	30 120	30 120	30 120	30 120	30 120	75	75	75	75	120	120	75
A	6	6	6	6	6	6	6	6	5	6	6	6	6
λ	.5	.5	.5	.5	.5	.5	.5	.5	.5	.25	.5	.5	.5

[1]For configurations 11 and 12, C_{n_r}, C_{Y_β}, and C_{n_β} were combined only in the same combinations as in configurations 1, 2, and 3.

TABLE II.– VALUES ASSUMED FOR AERODYNAMIC PARAMETERS

IN DETERMINATION OF DIRECTIONAL STABILITY

$\partial C_n/\partial\beta$ OF TEST AIRPLANES

Parameters	Airplane 1 (total, two tails)	Airplane 2 Configuration 1	Airplane 2 Configuration 2
Total vertical tail area, S_t, sq ft	91.0	26.58	23.72
Rudder area (aft hinge line), sq ft	33.6	8.65	8.30
Balance area, sq ft	9.56	1.97	1.96
Height (center-line stabilizer to tip along hinge line), ft	----	6.51	5.20
Height along hinge line, ft	8.43	----	----
Effective aspect ratio of vertical tail	1.56	2.47	1.77
l_t, ft	28.70	18.59	18.59
$\partial C_{N_t}/\partial\alpha_t$	.038	.049	.041
τ_r	.655	.585	.615
$d\delta_r/d\beta^\circ$ [1]	.620	1.060	.420
$\partial C_n/\partial\beta^\circ$ [2]	.000984	.001575	.000490
q_t/q	1.0	1.0	1.0

[1]In steady sideslips from flight data.

[2]$\partial C_n/\partial\beta^\circ$ is computed from the expression

$$\frac{\partial C_n}{\partial\beta^\circ} = \frac{(\partial C_{N_t}/\partial\alpha_t)\,\tau_r\,(q_t/q)\,S_t\,l_t\,(d\delta_r/d\beta^\circ)}{b_w S_w}$$

$C_{n_\delta} = -.00024\,C_L$

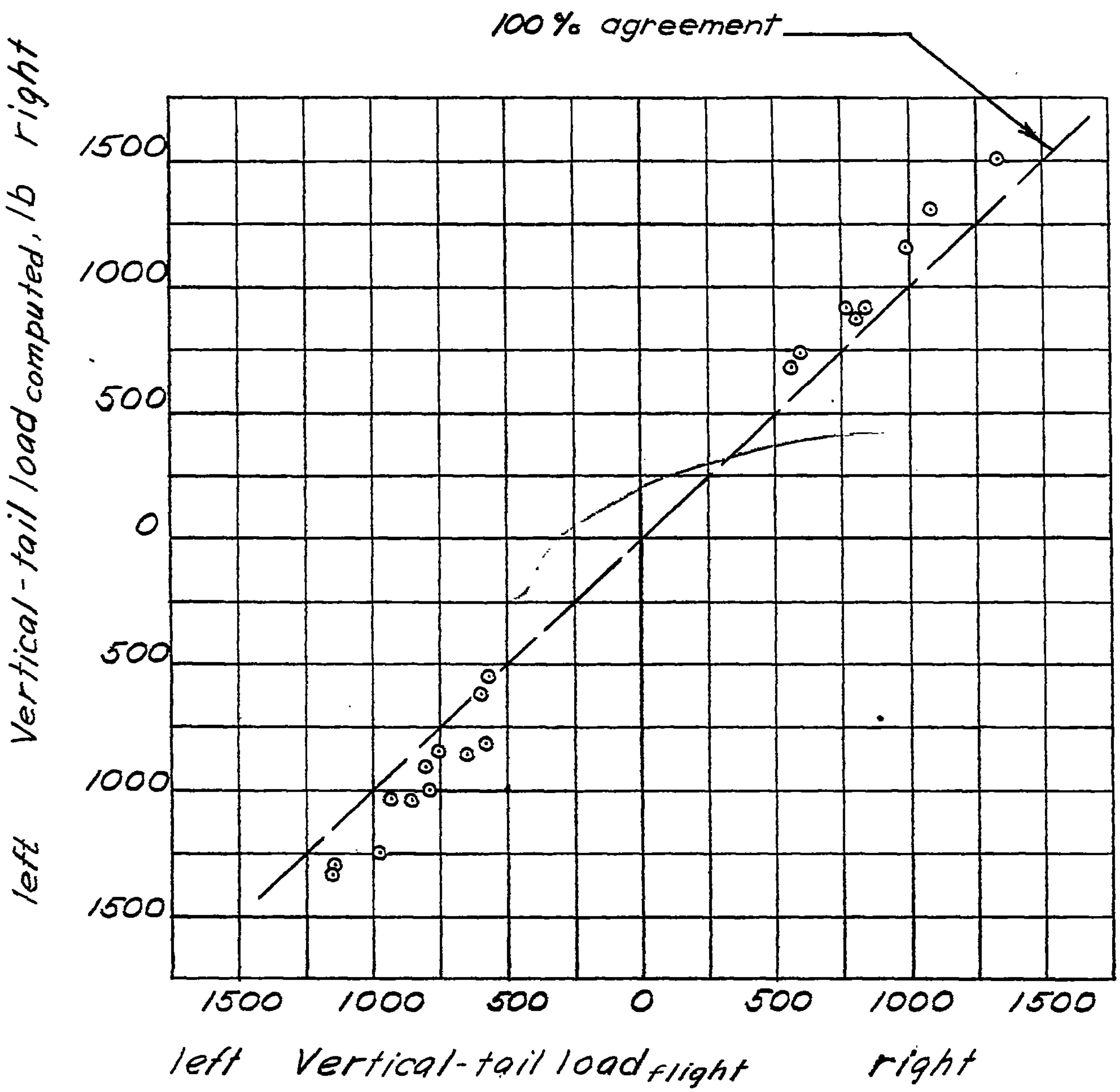

Figure 1.- Comparison of vertical-tail loads computed with measured values of β with vertical-tail loads measured in rolling pull-out maneuvers in flight. Airplane 3.

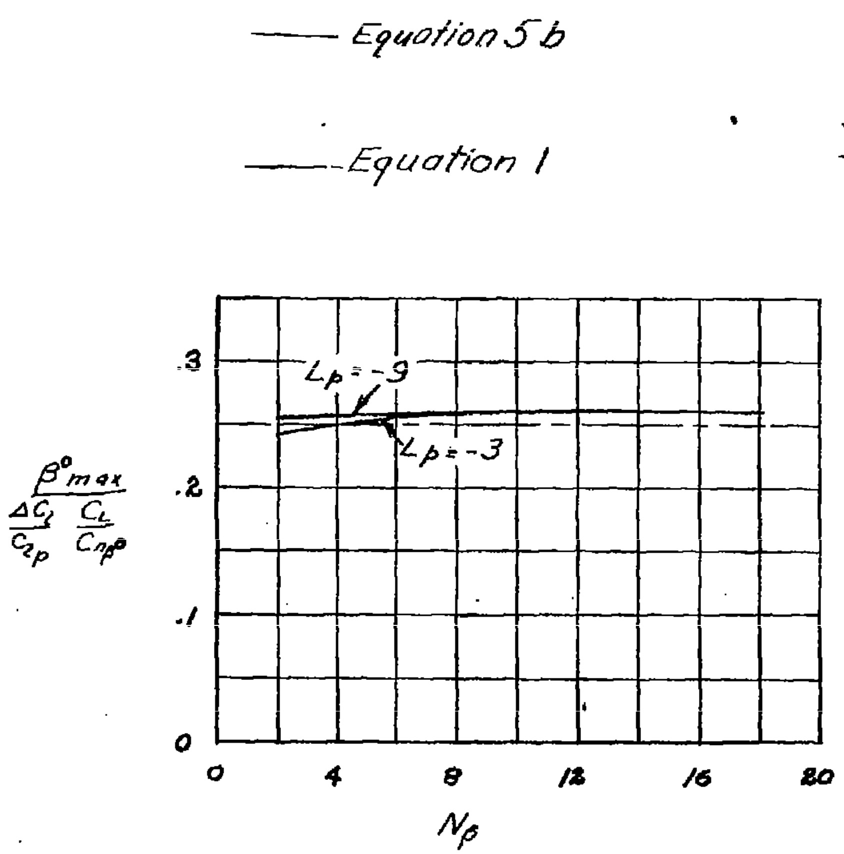

Figure 2.- Variation of the term $\beta^\circ_{max}/(\Delta C_l C_L / C_{l_p} C_{n_\beta}{}^\circ)$ with N_β for various values of L_p for an airplane in high-speed unaccelerated flight. $i_c = 0.143$, $N_r = -0.1264-0.0500\ N_\beta$, $Y_v = -0.117-0.0118\ N_\beta$.

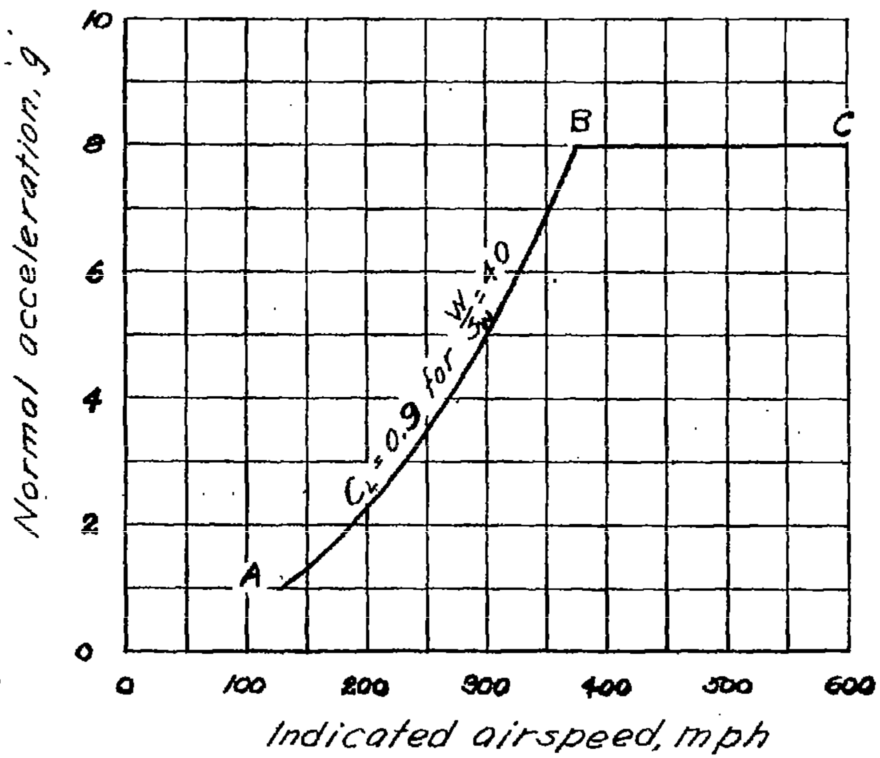

Figure 3.- Limits of normal accelerations and airspeeds covered by analysis.

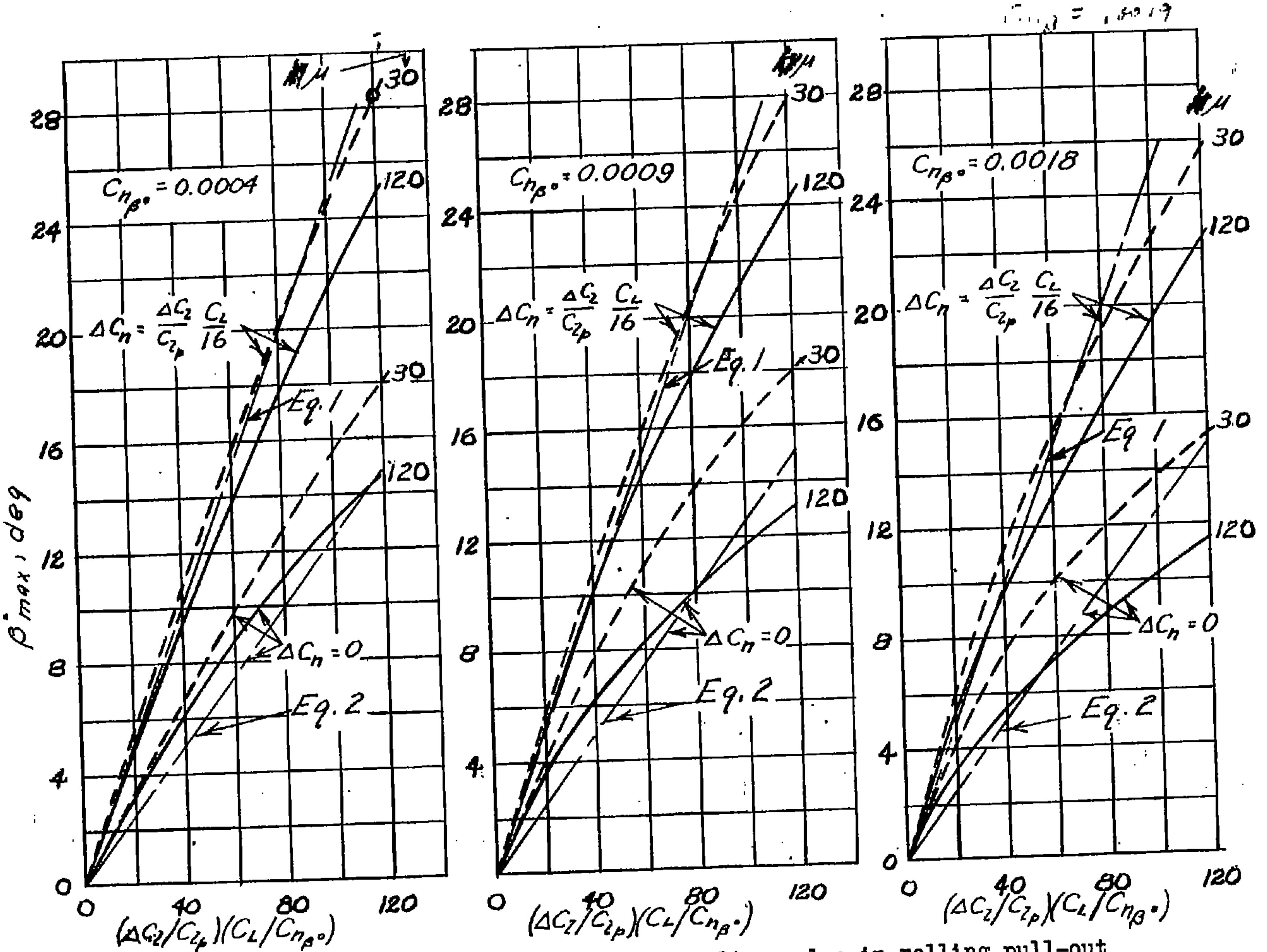

Figure 4a,b.- Design charts for maximum sideslip angles in rolling pull-out maneuvers. (a) $C_{l_{\beta}o}$ = -0.0010. Configurations 1,2,3 in Table I.

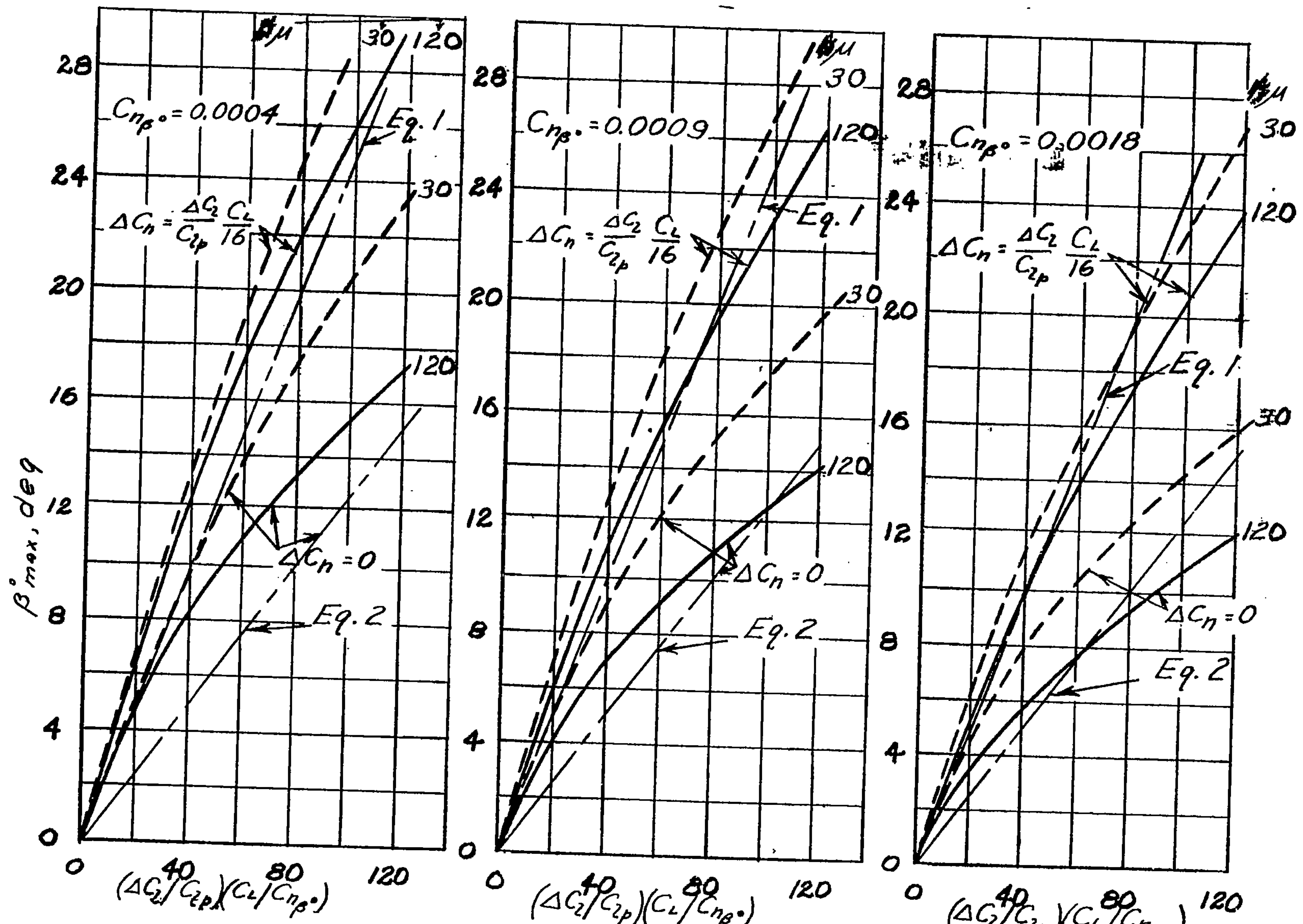

Figure 4.- Concluded. (b) $C_{l_{\beta o}} = 0$. Configurations 4,5,6 in Table I.

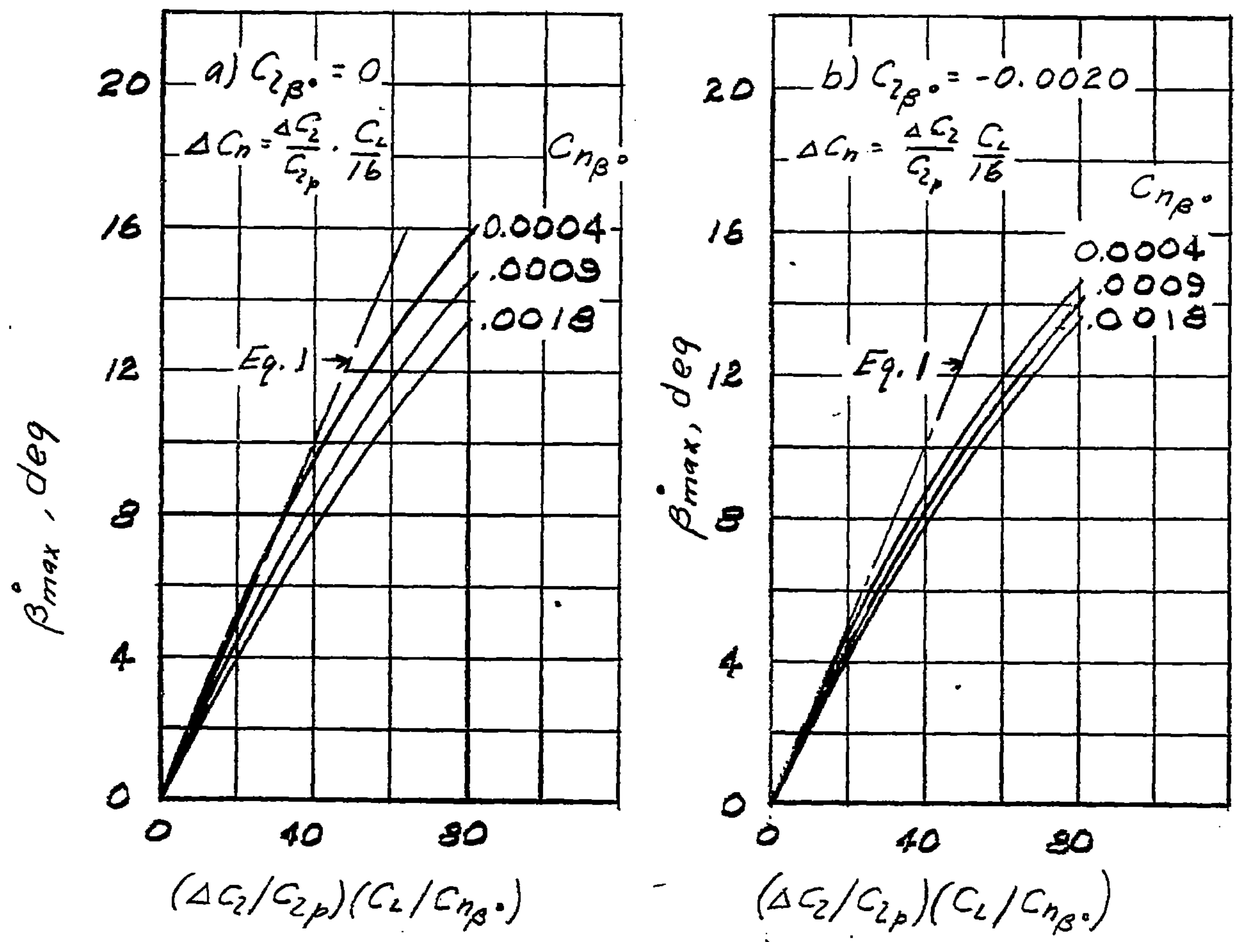

Figure 5.- Variation of the maximum angle of sideslip with $(\Delta C_l/C_{l_p})(C_l/C_{n_{\beta o}})$ for different values of $C_{n_{\beta o}}$ and $C_{l_{\beta o}}$. Configurations 11,12 in Table I.

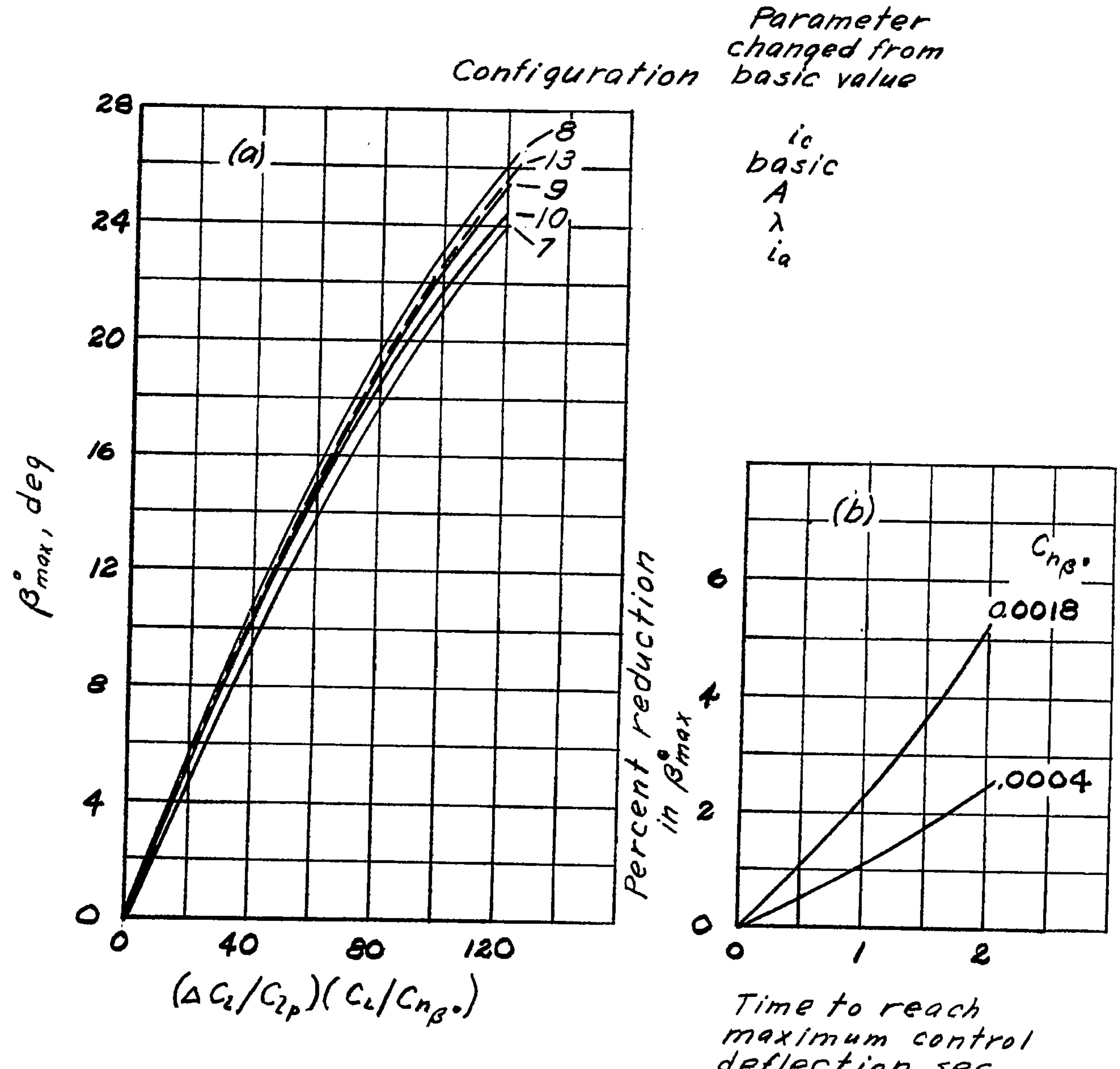

Figure 6.- Effect of independent changes in several variables on the maximum sideslip angle.

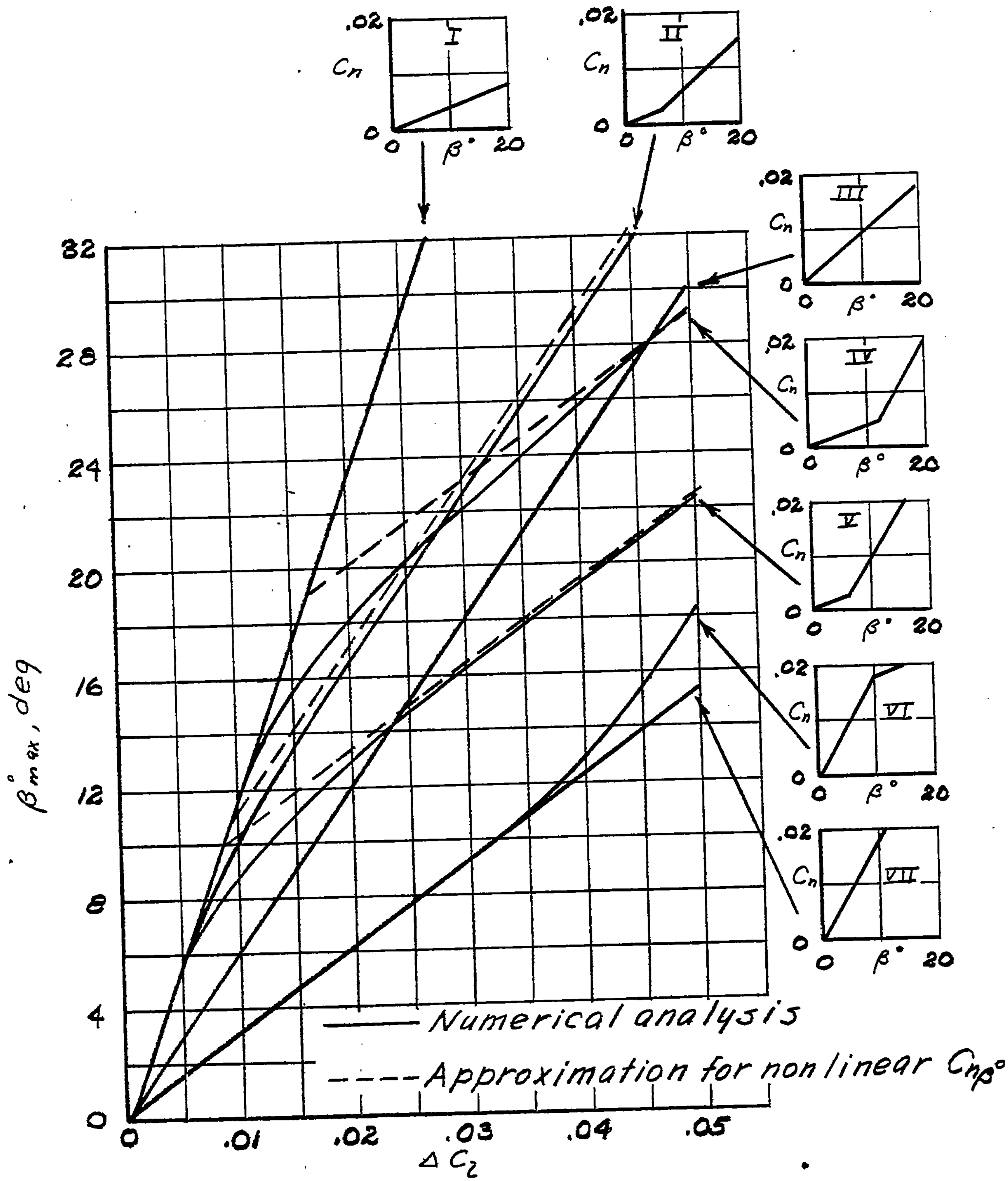

Figure 7.- Effect of nonlinear variations of C_n with $\beta°$ on the maximum sideslip angle.

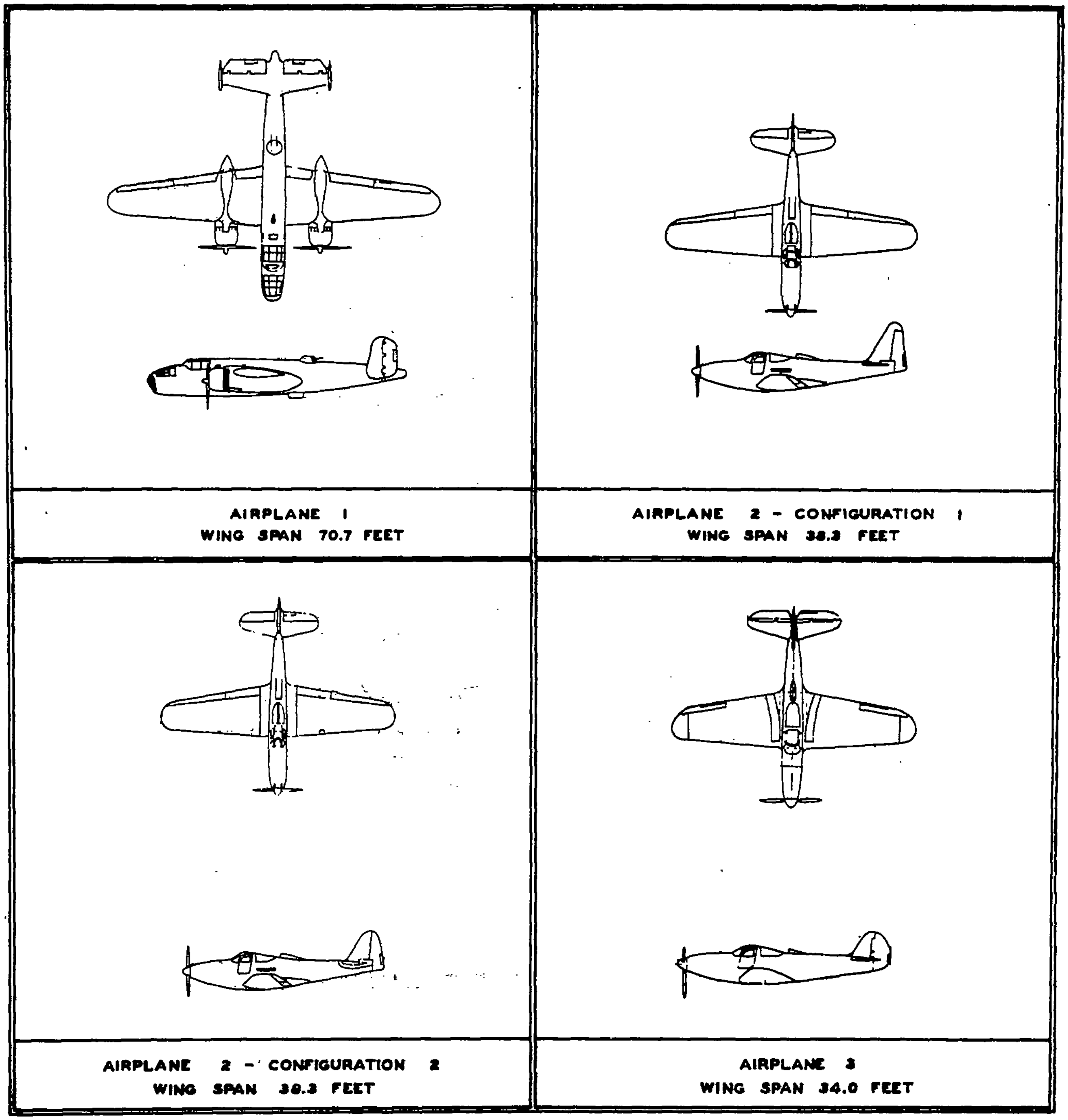

FIGURE 8.- TWO-VIEW DRAWINGS OF THE AIRPLANES TESTED IN FLIGHT

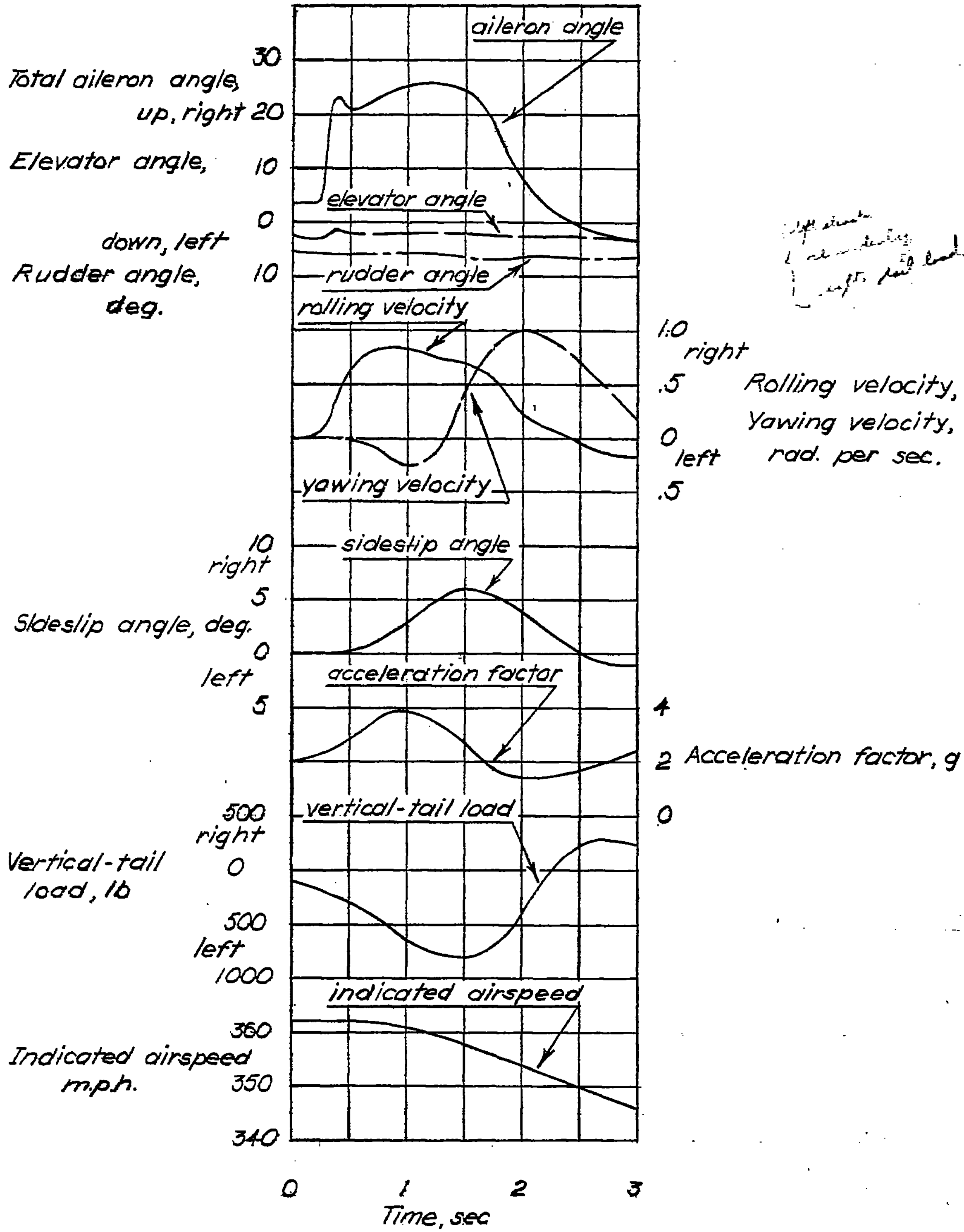

Figure 9.- Typical time history of a roll out of a steady turn of airplane 3.

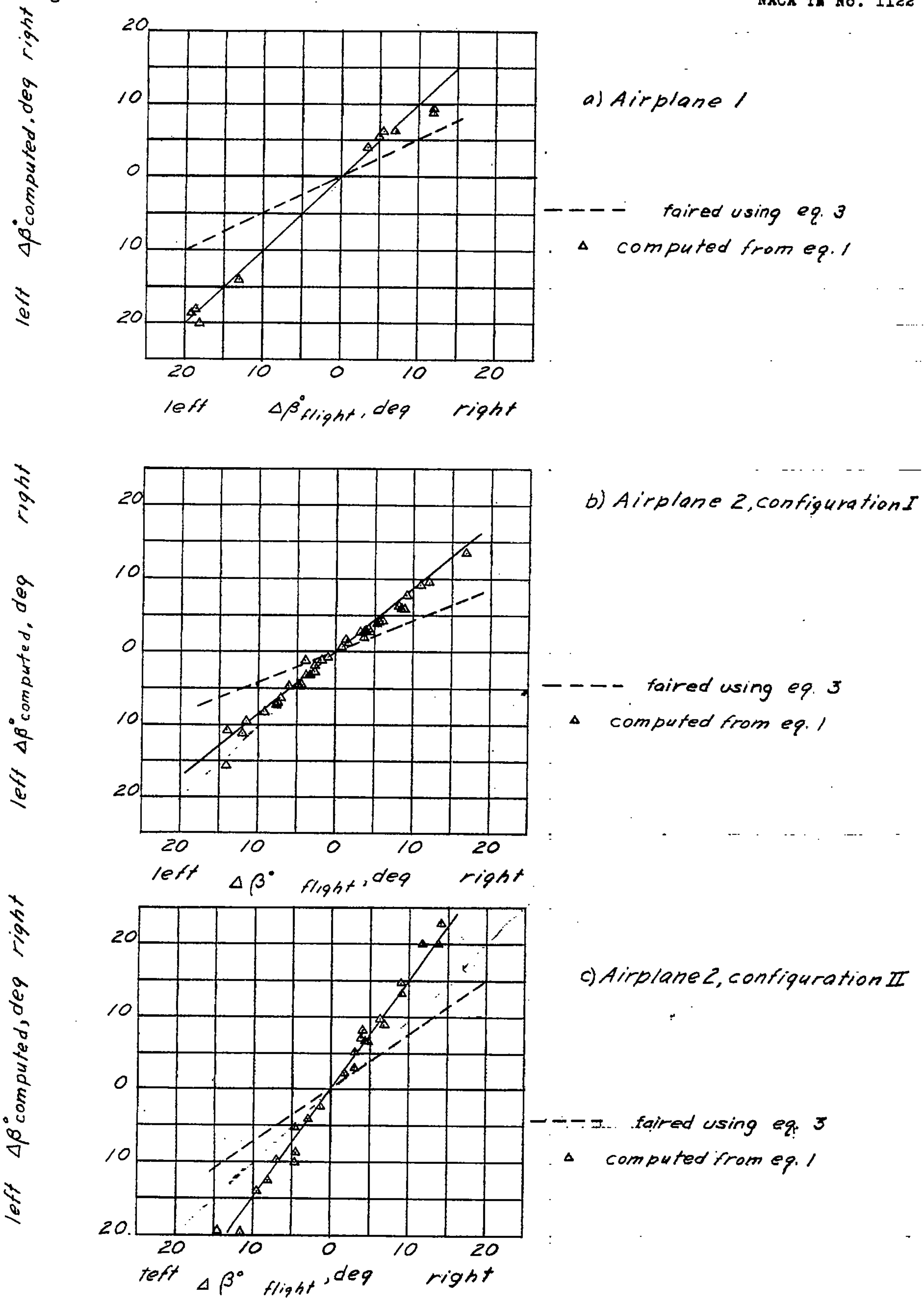

Figure 10.- Comparison of calculated values of Δβ° with values measured in rolling pull-out maneuvers in flight on several airplane configurations.